Acoustic Remote Sensing of Planetary Boundary Layer Dynamics near Ross Island, Antarctica*

ZHONG LIU AND DAVID H. BROMWICH

Byrd Polar Research Center and Atmospheric Sciences Program, The Ohio State University, Columbus, Ohio

(Manuscript received 22 October 1992, in final form 20 April 1993)

ABSTRACT

The blocking effect of Ross Island and Hut Point peninsula, Antarctica, has been investigated since the early part of this century. Due to lack of continuous measurements of boundary-layer winds, the investigations were limited to an overall description of the blocking effect with no information on the diurnal variation or the detailed vertical structure of the approaching airflow.

An acoustic sounder (sodar) was deployed during the 1990/91 austral summer season at Williams Field in the upwind area south of Ross Island, Antarctica. Such equipment can continuously measure three-dimensional winds from a few tens of meters above the surface up to an altitude of several hundred meters, thus providing a new opportunity to study the dynamics of the stably stratified planetary boundary layer.

In addition to confirming earlier work, the sodar winds show a significant diurnal variation of the blocking effect, which amplifies with height. Such variation is dominated by the changes in the upstream air mass in which katabatic airflow from Byrd, Mulock, and Skelton glaciers plays a central role.

Through case studies, the breakdown of the prevailing wind regime in the Ross Island area was associated with the influence of meso- and synoptic-scale pressure gradients on the katabatic airflow approaching from the south and with very localized geostrophic winds deflected around the topography of Ross Island.

1. Introduction

Ross Island, Antarctica, is located at the northwestern edge of the Ross Ice Shelf (Fig. 1a). Three peaks (Fig. 1b) of more than 2000-m elevation, Mts. Erebus, Terra Nova, and Terror, form this steep terrain feature, which presents almost a vertical wall to the prevailing southerly winds. Windless Bight (Fig. 1b) is formed by the southern edge of Ross Island. Since Windless Bight was explored by the British expeditions of Robert F. Scott (1901–04 and 1910–13) and Ernest H. Shackleton (1907–09 and 1914–17), a number of studies related to the blocking effect of Ross Island and Hut Point peninsula have been conducted. Sinclair (1982) investigated airflow around and over Hut Point peninsula (Figs. 2a,b) based on traverse and surface observational data. Figure 2a displays the streamlines of prevailing wind flow around Ross Island as deduced from the directions of the most frequent wind. Similarly, Fig. 2b illustrates the airflow during strong winds as inferred from directions of the strongest wind and from sastrugi orientations. Comparison of the two streamline depictions illustrates the breakdown of the blocking effect of Hut Point peninsula with strong winds. Schwerdtfeger (1984) discussed the effect of Ross Island on the prevailing southerly winds when the near-surface air is stably stratified. Following Schwerdtfeger's idea, Slotten and Stearns (1987) investigated the dynamics and kinematics of the atmospheric surface layer around the Ross Island area using an array of six automatic weather stations (AWS) and demonstrated the existence of the island blocking. O'Connor and Bromwich (1988) modeled the surface airflow past Ross Island using a two-dimensional, steady, frictionless, irrotational, incompressible flow past an obstacle based upon an island height contour. The model results reproduced the light wind zone in Windless Bight as a result of airflow around the island. From their analysis of McMurdo radiosonde data, it was inferred that Hut Point peninsula is a key factor for the appearance of a clockwise rotation of the horizontal wind direction with height under stably stratified and moderate wind speed (<10 m s^{-1}) conditions.

The Froude number (O'Connor and Bromwich 1988), the ratio of the kinetic energy of the approaching wind to the potential energy required to lift an air parcel from the surface to the height of the obstacle, is frequently used to explain blocking phenomena under statically stable conditions. The Froude number equation can be written as

$$\mathrm{Fr} = U_0\left(\frac{gH\Delta\theta}{\bar{\theta}}\right)^{-1/2},$$

* Contribution 844 of Byrd Polar Research Center, The Ohio State University.

Corresponding author address: Dr. David H. Bromwich, Byrd Polar Research Center, The Ohio State University, 108 Scott Hall, 1090 Carmack Rd, Columbus, OH 43210-1002.

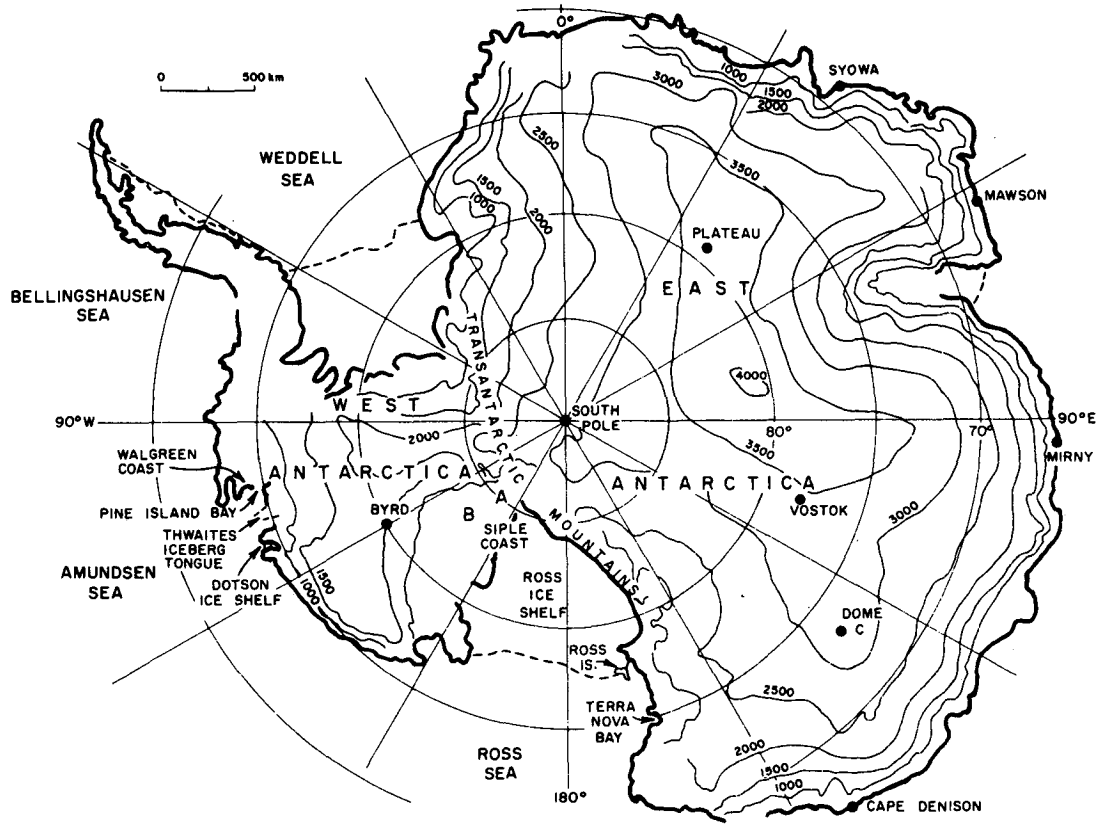

FIG. 1a. Location of Ross Ice Shelf and Ross Island in Antarctica (from Parish and Bromwich 1986).

where U_0 is the approaching wind speed, g is the acceleration due to gravity, H is the height of the obstacle, $\Delta\theta$ is the potential temperature difference between the surface and the top of the obstacle, and $\bar{\theta}$ is the vertically averaged potential temperature over this layer. Kitabayashi (1977) studied the upstream blocking of a stable boundary-layer flow by a 200-m-high ridge line in Japan. The critical Froude number (=2.3) was derived from analyses of meteorological and wind tunnel data. The Froude number calculated from McMurdo Station observations during March–October 1979 (O'Connor and Bromwich 1988) was 1.4 (<2.3) for airflow around and 2.8 (>2.3) for airflow over Hut Point peninsula. Apparently, the critical Froude number from Kitabayashi can be used to monitor the breakdown of the blocking effect of Hut Point peninsula.

These previous studies did not address the diurnal variation of the blocking effect nor the source of the prevailing airflow. In addition, the studies did not provide a detailed description of the vertical structure of the approaching airflow because they mostly relied on surface weather observations from traverse parties, manned stations (e.g., McMurdo Station, Scott Base), and AWS. These data usually provide information on the behavior of the lowest few meters of the atmosphere. Radiosonde data collected at McMurdo Station describe the vertical structure of the atmosphere but are not suitable for detailed study of the planetary boundary layer, because of the area's complex topography and their poor height resolution and inconsistent launches. An acoustic sounder (Fig. 3), or sodar (an abbreviation for sonic detection and ranging), easily overcomes these limitations by providing continuous three-dimensional wind profiles up to an altitude of several hundred meters. In the complex topographic setting of the Ross Island area, a sodar is an ideal tool for resolving the vertical structure of the boundary layer.

This paper will address three issues: first, description of sodar utilized and the site investigated; second, the blocking effect and its diurnal variation based on sodar wind data; and finally, northwest wind events, which often caused adverse weather during the campaign and represent a breakdown of the prevailing wind regime.

2. Sodar configuration and site selection

The three-dimensional wind is derived from Doppler analysis of the returned acoustic signals. The three-axis, monostatic sodar (Fig. 3) is composed of three acoustic transducers mounted at the focal points of three parabolic reflectors. These assemblies are each enclosed in

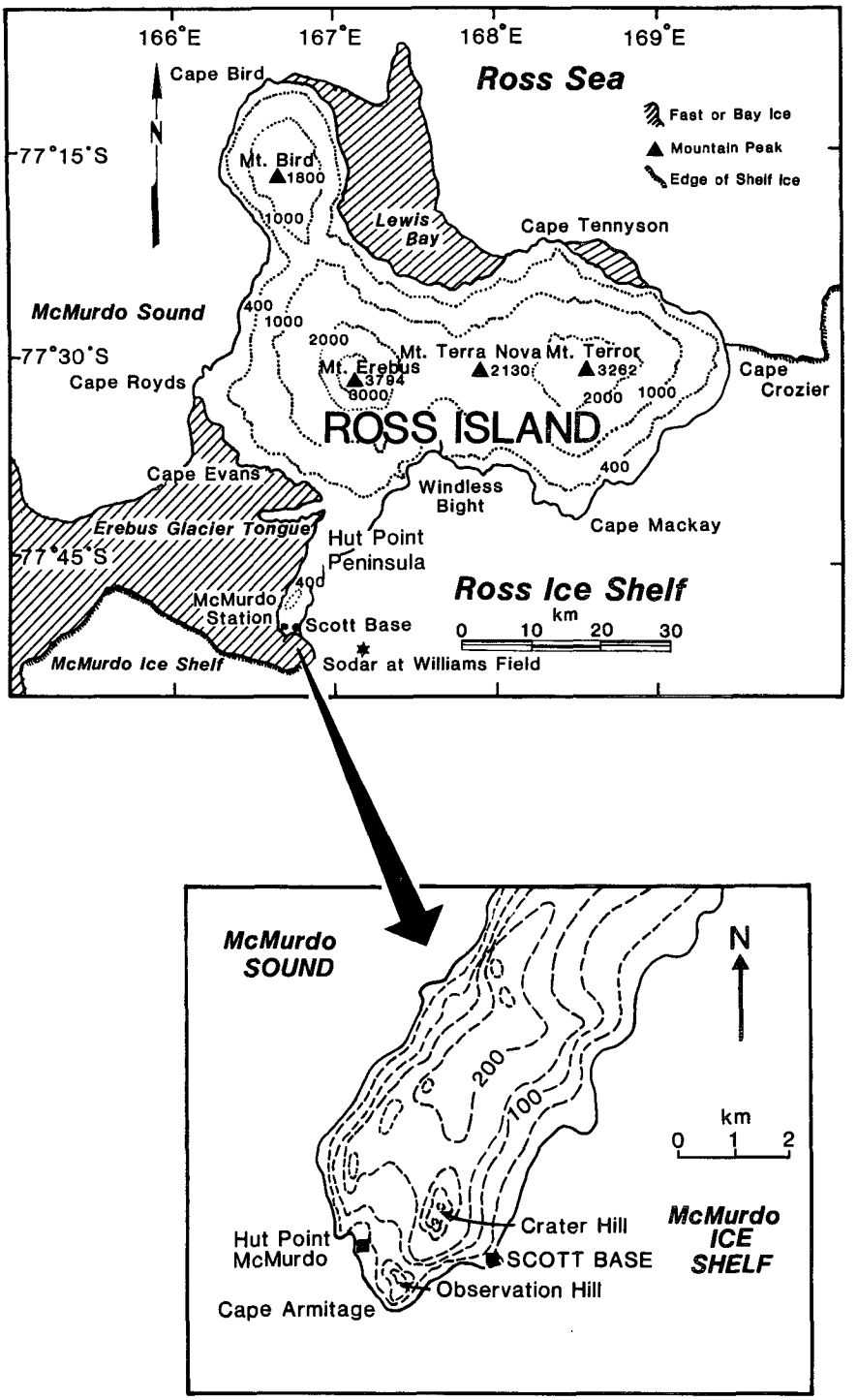

FIG. 1b. Topographic maps of Ross Island and the southern end of Hut Point peninsula, adapted from O'Connor and Bromwich (1988) and Sinclair (1982). The sodar was located at Williams Field and is marked by an asterisk. Dashed elevation contours are in meters.

a protective fiberglass cylinder that has a layer of acoustic dampening foam on its inside surface. Each one of these three shielded transceivers is referred to as a leg.

The legs are mounted in line on a rack at specific orientations. The center leg lies along the vertical axis. The next leg lies in the plane formed by the vertical

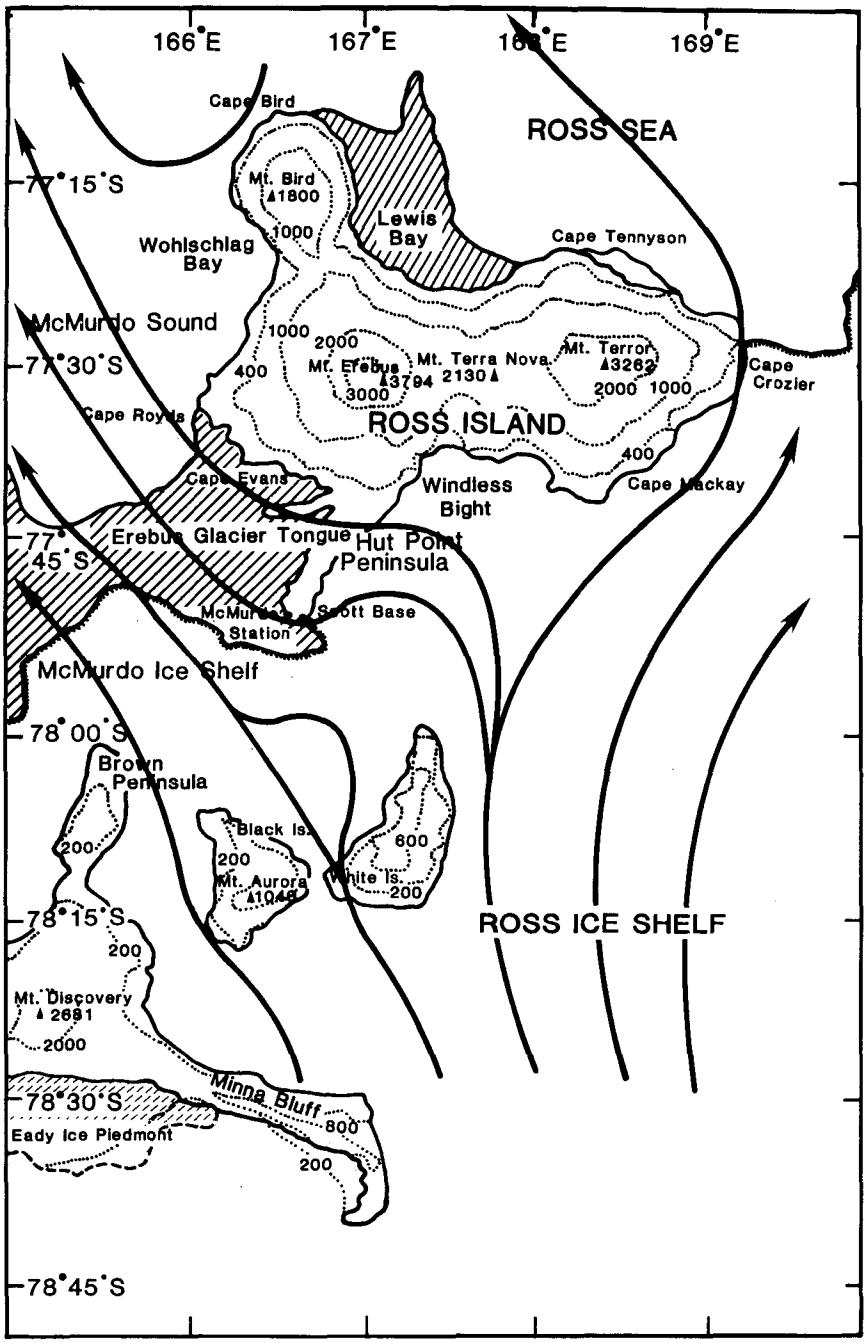

FIG. 2a. Streamlines of prevailing surface airflow around Ross Island. Elevation contours (dashed) are in meters. [Modified from Sinclair (1982) and Stearns and Weidner (1990).]

axis and the long axis of the rack but is oriented at an angle of 22.5° away from vertical. The last leg is also tilted at an angle of 22.5° but in a plane normal to the plane containing the axes of the other two legs.

This particular sodar operates at an acoustic frequency of 2250 Hz. The sodar collects data by transmitting a 2250-Hz pulse of selected duration in a round-robin fashion from each of the legs; the transmitting transducer then switches to receiving mode. Based on the known frequency, pulse duration, and leg orientation, a specialized signal processing card located in a microcomputer expansion slot calculates the three-dimensional wind values from the three monostatic returns. The data are passed to the computer and written to disk for subsequent analysis.

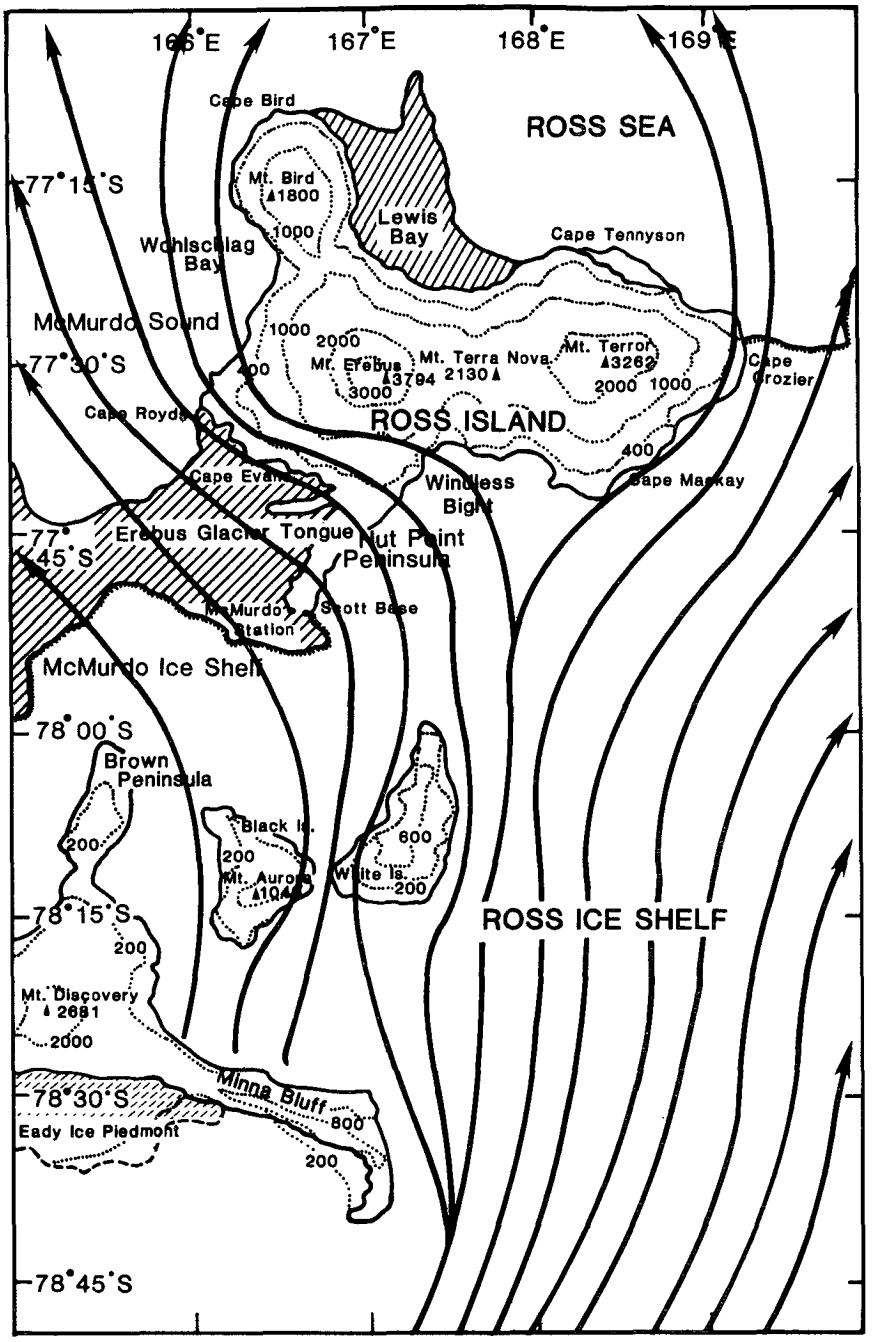

FIG. 2b. Streamlines of strong surface airflow around Ross Island as deduced from the directions of the strongest wind at 17 sites. [Modified from Sinclair (1982) and Stearns and Weidner (1990).]

Since 1975, several investigators (Hall and Owens 1975; Neff 1981; Mastrantonio et al. 1988; Liu and Bromwich 1992; Liu et al. 1991; Argentini et al. 1992) have successfully deployed sodars for boundary-layer studies in Antarctica. The sodar (Fig. 3) used in this campaign is of a special configuration customized by Radian Corporation especially for operations in the rigorous environment of Antarctica. (Temperatures ranged from −32° to +3°C, and wind speeds up to 18 m s^{-1} were experienced.) The unit is compact relative to the most common sodar designs and is constructed of durable lightweight materials. It is also mounted on skis for portability.

The campaign lasted from 19 October to 5 November 1990. The sodar was set up at Williams Field (Fig. 1b) on the Ross Ice Shelf and was run continuously to

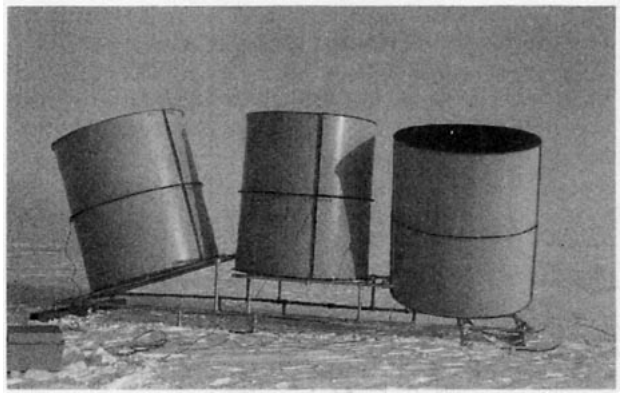

FIG. 3. The three-axis, monostatic sodar used in the 1990 campaign. The cylinders are 6 ft high.

record three-dimensional wind profiles above the ice shelf. In comparison with other surface camps in Antarctica, Williams Field is relatively large. To minimize the effects of camp buildings and vehicle noise, the sodar was sited several hundred meters upwind from the camp (Fig. 3). The runway south of Williams Field was not in operation during the campaign. No consistent noise signals showed up on the sodar backscatter except during occasional vehicle and helicopter passages.

3. Blocking effect and source of the prevailing wind

a. Resultant wind analysis

The vertical structure of the horizontal wind in the Ross Island area was investigated by O'Connor and Bromwich (1988) based on rawinsonde data at McMurdo Station. They classified these data into two categories: (a) surface wind direction lying between north and east and a wind speed of at least 5 m s^{-1}, and (b) wind direction from southeast to southwest and a speed greater than or equal to 5 m s^{-1}. Their Table 2a shows that for the first category both the horizontal resultant wind speed decreases and the resultant direction turns clockwise with height. A shallow inversion layer was found at the surface. They concluded that these phenomena are associated with the blocking effect of Hut Point peninsula on airflow because the pileup of air creates a pressure gradient directed away from the peninsula.

To verify this, the horizontal resultant wind speed and direction profile was derived from sodar wind measurements at 15-min intervals during the campaign (Fig. 4). In Fig. 4, the wind direction rotates clockwise as height increases to 325 m and becomes uniform above that height. A low-level jet (Stull 1988) is located at 75-m height, due to the blocking and frictional slowing near the surface, and wind speed decreases with height above that. This low-level clockwise rotation of wind direction and the low-level jet confirm the blocking effect of Hut Point peninsula. Calculation of the Froude number was difficult for this study because of the lack of continuous measurements of boundary-layer temperatures. During the period, 23 sounding balloons were launched at the sodar site under fair weather conditions (no strong winds or heavy precipitation). The balloons followed the prevailing wind trajectories toward Hut Point peninsula. Based on the assumed 3 m s^{-1} ascent rate, the balloons were still south of the peninsula at 200-m altitude. In comparison, the radiosondes released at McMurdo Station normally had drifted behind the ridge by this time. The launches were scattered throughout the day during the campaign. The average potential temperature difference (derived from the sounding data) between the ice shelf and 200-m height was 6.7 K ± 5.0 K (one standard deviation). If the maximum and minimum surface resultant wind speeds (2.6 and 1.3 m s^{-1}, respectively, derived from a recording anemometer at the sodar site) and the average potential temperature (255 K, derived from the sounding data and measurements at the sodar site at 1.5 m above the surface and at 3-h intervals) are used, the calculated Froude numbers are 0.36 and 0.18, respectively. These numbers are far less than Kitabayashi's critical Froude number (2.3) and that (1.4) from O'Connor and Bromwich (1988) for airflow around Hut Point peninsula. In the latter situation, the wind speed (6.8 m s^{-1}) was higher and the potential temperature difference (2.9 K) was smaller than the corresponding values used in the present calculation. This result explains the persistent blocking by the peninsula during the campaign.

Examples of the blocking effect of Hut Point peninsula and its breakdown are given in Figs. 5a and 5b,

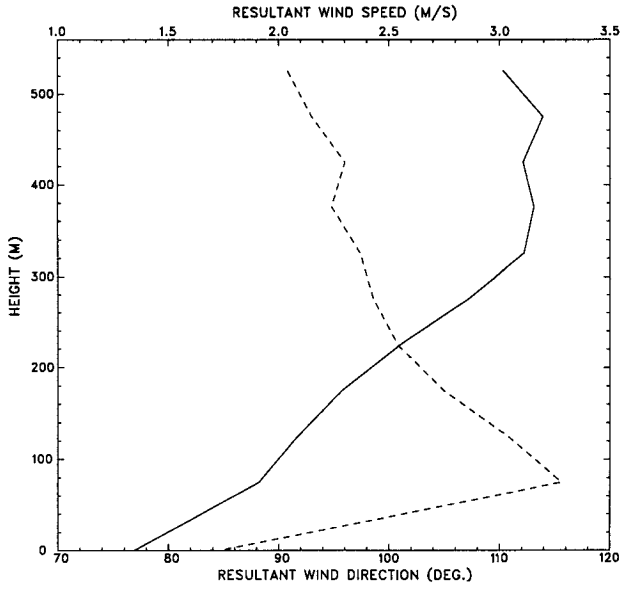

FIG. 4. The profiles of resultant wind direction (solid) and resultant wind speed (dashed).

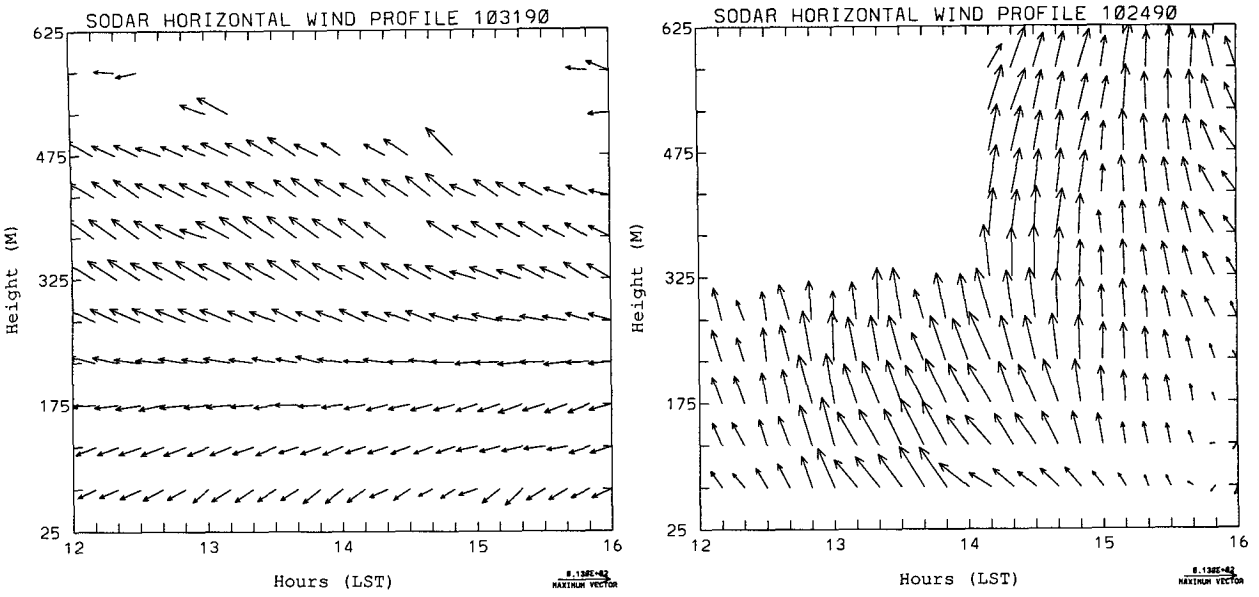

FIG. 5. (a) An example of the blocking effect of Hut Point peninsula from 1200 to 1600 LST 31 October 1990. (b) An example of airflow over the peninsula from 1200 to 1600 LST 24 October 1990.

respectively. In Fig. 5a, below 225-m height, which is near the height of the ridge line of Hut Point peninsula, the wind direction turns clockwise from northeasterly at the surface. Above the 225-m height, the flow is uniformly from the southeast. The situation for flow over the peninsula under strong wind conditions is shown in Fig. 5b. Wind speeds of greater than 10 m s^{-1} are dominant. Along the vertical direction, the wind directions show little shear.

b. Hourly resultant wind analysis

One of the unanswered questions in the previous studies is the diurnal variation of the blocking effect. Continuous wind measurements from the sodar provide an opportunity to study this aspect. Figures 6 and 7 were derived from hourly resultant wind vectors that were smoothed by 3-h means. Figure 6 shows the 3-h resultant wind direction profile as a function of local standard time (LST). The diurnal evolution of the blocking effect of Hut Point peninsula can be described as, in general, existing throughout the day with a well-defined clockwise wind direction rotation between 0800 and 2000 LST. A less well defined wind direction rotation appears during the rest of the day, especially at about 0600 LST. Examination of the directional constancy (ratio of resultant wind speed to mean wind speed) profile (Fig. 7) shows a decreasing trend at most levels appearing after 1800 LST with a minimum around 0900 LST and an increasing trend thereafter. Therefore, the decrease of the directional constancy as a result of more variable wind directions is probably the main reason for the small directional shear in the early morning when the strong inversion layer developed. Although a shallow (less than 50 m in height) convective layer was present during the daytime hours for most of the period, as shown by temperature data from sounding balloons released from the sodar site, the blocking effect was still a prominent feature. This is because insolation of the high-albedo ice shelf surface did not produce marked heating and the convective

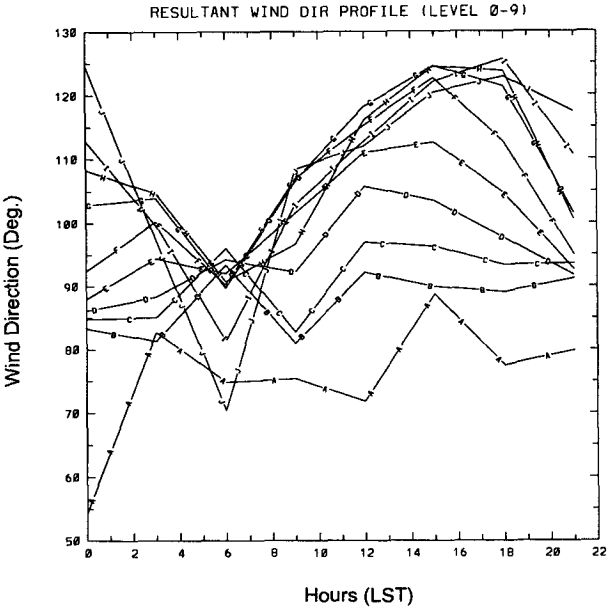

FIG. 6. The 3-h resultant wind direction profile as a function of time. Line A represents the surface level, while lines B, C, D, E, F, G, H, I, and J represent the 75-, 125-, 175-, 225-, 275-, 325-, 375-, 425-, and 475-m heights, respectively.

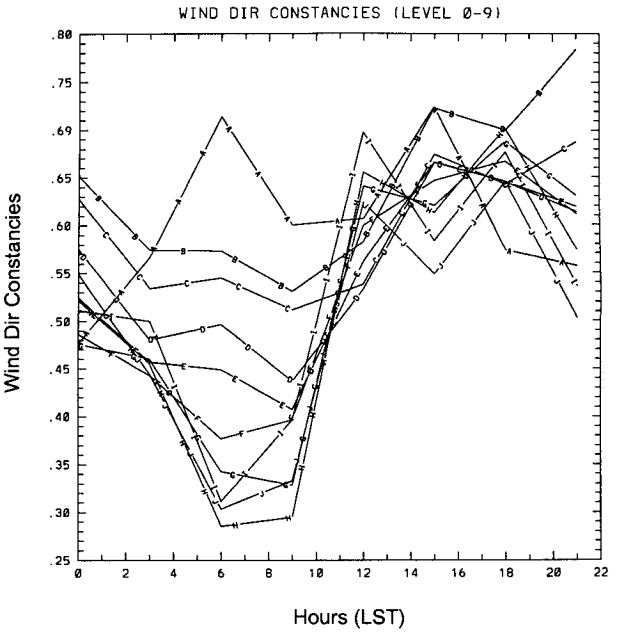

FIG. 7. The 3-h wind directional constancy profile as a function of time. See caption to Fig. 6 for symbol explanations.

mixing layer was too shallow to destroy the inversion layer; therefore, the inversion layer was always the dominant feature of the boundary layer.

In Fig. 6, the wind directions at each level below (above) the ridge line are uniform (varying) during the daytime. During the early morning, the wind directions are uniform for the entire layer. Such phenomena can be described using the Froude number concept. Figure 8 shows the evolution of the surface Froude number calculated from the sounding balloon and surface observation data at the sodar site during the campaign. The variation of Froude number reflects the diurnal changes of the boundary layer with high Froude numbers during daytime (higher wind speeds and smaller air temperature differences between the ridge and the ice shelf) and low values during nighttime (low wind speeds and larger air temperature differences). The maximum Froude number (0.56) is far less than that (1.4) from O'Connor and Bromwich (1988) for surface airflow around Hut Point peninsula. This is consistent with the previous discussion about the resultant wind direction profile. Above the surface, the Froude numbers can only be qualitatively estimated from Fig. 6 due to the shortage of vertical temperature profiles. In Fig. 6, the small diurnal variation of the wind direction below the ridge line implies that the Froude number of the flow at this level is generally below the critical value for flow over this level. Through the examination of the Froude number equation, this is possibly due to the fact that the decreasing lifting height and potential temperature difference are compensated by the decreasing wind speed with height. During the nighttime, the decreasing directional separation for all the levels is because of the decrease of the Froude number due to decreasing wind speeds and increasing difference of potential temperature, decreasing wind directional constancies, and a more laminar flow pattern. As a result, the airflow can be more easily deflected by the local and surrounding topography.

The 3-h resultant wind speed profile was also derived (Fig. 9) to show the diurnal evolution of the low-level jet. In general, the jet strengthens from 0900 LST to a maximum around 1500, and weakens from 1500 to the minimum near 0900 LST. The pattern of the low-level jet is less well defined during the daytime (from 1000 to 1700 LST) due to increased turbulent mixing from insolation heating and from mechanical shear generation due to stronger low-level winds; it is well-defined during nighttime (from 1800 to 0900 LST) as the flow tends to be more laminar due to gradually strengthening boundary-layer stability from net long-wave radiational heat loss.

c. *Propagation of the katabatic winds*

As shown by Fig. 9, the whole boundary layer acts like the low-level jet with a similar diurnal variation. This kind of variation is not like that occurring in mid-latitudes due to downward momentum flux transfer from the free atmosphere because the momentum fluxes, in fact, are downward beneath the low-level jet

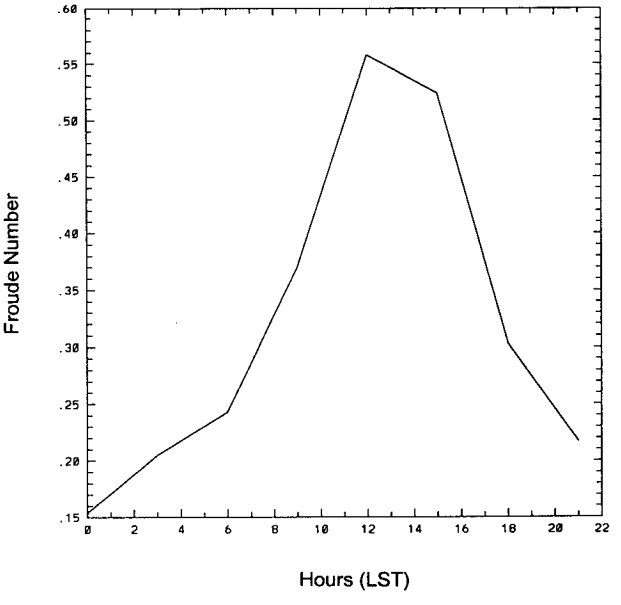

FIG. 8. Evolution of the surface Froude number derived from balloon sounding and surface observational data at the sodar site. The surface temperatures were measured at the 1.5-m height at 3-h intervals during the campaign. The average air temperature [=254.9 K ± 2.2 K (one standard deviation)] at the 200-m height was used for calculation of potential temperature difference. Wind speeds were derived from the recording anemometer at the sodar site.

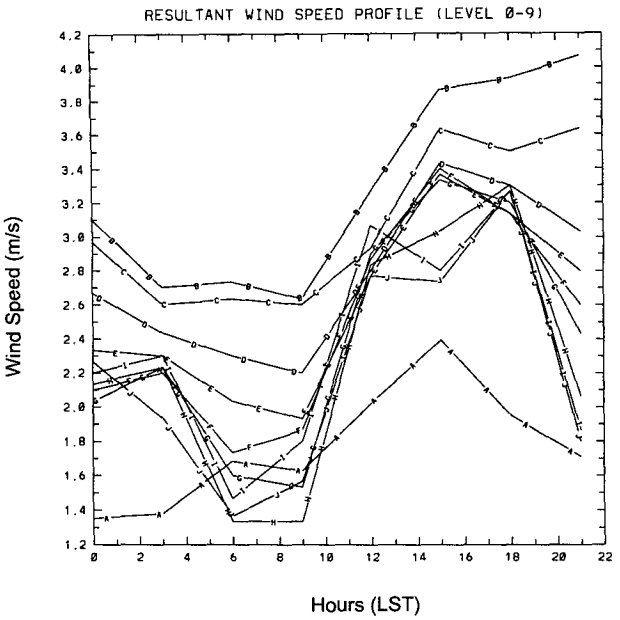

FIG. 9. The 3-h resultant wind speed profile. See caption to Fig. 6 for symbolism explanation.

and upward above it. Recent numerical simulations (Parish and Bromwich 1987, 1991) indicate that the katabatic winds, a climatic feature in Antarctica, are highly irregular over the continent and characterized by confluence zones near the coast where the drainage flow is intensified and more persistent. Their simulations suggest that the airflow passing through the Ross Island area is supplied mainly by enhanced katabatic drainage from Byrd Glacier and secondarily drainage from Mulock and Skelton glaciers (see Fig. 10). Bromwich (1991) constructed a yearly average of the sea level isobars, surface isentropes, and resultant winds over the western half of the Ross Ice Shelf. Streamlines, drawn from the resultant wind directions in Fig. 9 of his paper, again suggest the dominant contribution of katabatic airflow from Byrd, Mulock, and Skelton glaciers to the prevailing wind regime near Ross Island. Recent model simulations with zero large-scale pressure gradients (Bromwich et al. 1994) show the dynamics of the katabatic drainage flows from the three glaciers, which can be thought of as part of the circumpolar "easterlies." In general, the katabatic drainage flows come down from the mountains, lose the downslope buoyancy force over the flat ice shelf, and become pseudoinertial flows. These inertial flows turn to the left because of the Coriolis force and eventually reach the mountains. Once this stable air piles up against the mountains, a pressure gradient force forms that is directed away from the mountains. Finally, a barrier wind forms due to the balance between Coriolis and pressure gradient forces. Though the above model simulation was conducted for austral winter season, numerical study by Parish et al. (1993) suggests that the katabatic wind is a robust feature of the Antarctic boundary layer even during midsummer months. At these times, the

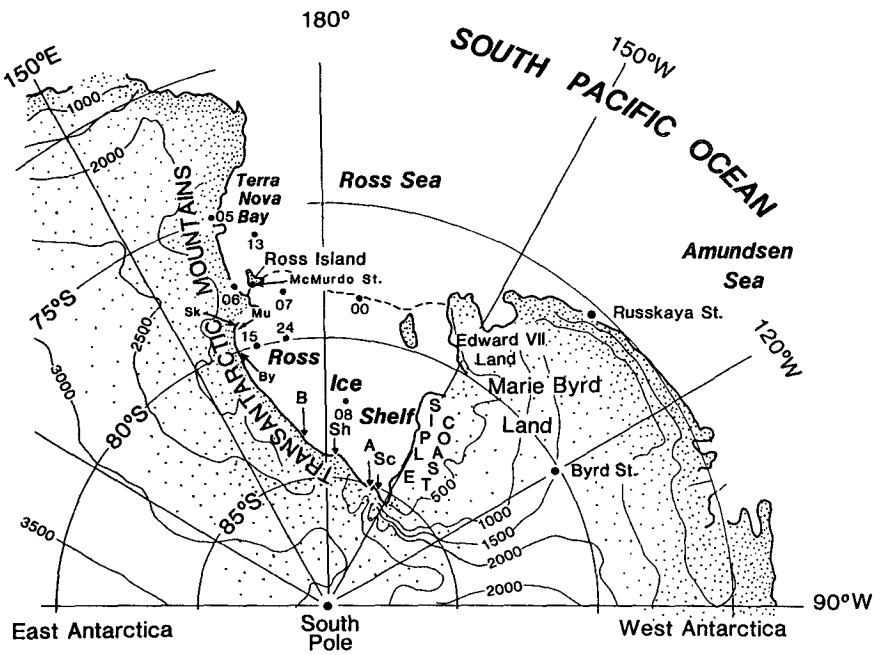

FIG. 10. Location map of automatic weather stations (dots with numbers) during the 1990 campaign. Just to the south of Ross Island, Mu, Sk, and By denote Mulock, Skelton, and Byrd glaciers [adapted from Bromwich et al. (1992)].

katabatic wind decreases considerably during the middle of the day and wind speeds at coastal sites show significant diurnal variation.

One result of this propagation scenario is that boundary-layer events in the Ross Island area are probably caused by variations of the drainage flows from these glaciers. To further verify this, wind data from AWS 15 and 07 were used (see Fig. 10). The reason for using AWS 15 is its closeness to Byrd Glacier and thus its measurement of the drainage flow contribution mostly from that glacier to the main stream as a function of time; AWS 07, which is located to the southeast of Ross Island, is for additional verification of the tributary effect due to the blocking effect of Ross Island. The use of AWS 15 may somewhat ignore the additional contributions of drainage flows from Mulock and Skelton glaciers, but it is the only station that is available for this study. The resultant wind speeds and directions for both stations based on 3-h observations during the campaign (Keller et al. 1991) were calculated.

Figure 11 shows that the surface wind direction at AWS 15 turns clockwise as the wind speed increases. This implies increasing influence of katabatic drainage from Byrd Glacier. Another feature of the surface wind at AWS 15 is the diurnal variation. Notice that the maximum wind speed occurs at 0900 LST. Because the minimum surface temperatures usually occur in the early morning, as does the drainage flow maximum, it is likely that the drainage flow from Byrd Glacier takes 4.5 h (90 km/20 km h^{-1}) to reach AWS 15 if deceleration of the drainage flow, due to decreasing negative buoyancy forcing and friction, is taken into account. A similar diurnal variation of wind speed is also found at AWS 07 (Fig. 11b). The maximum that occurs at 1500 LST agrees with that of the surface wind at Williams Field. In fact, Figs. 2a and 2b show that both Williams Field and AWS 07 are under the influence of the same southerly airflow that parts to the south of Ross Island and are roughly within the same radial distance (about 250 km) from AWS 15. From Fig. 11b, the time difference between the maxima at AWS 07 and 15 is about 30 h. Thus the average propagation speed is about 8.3 km h^{-1} (250 km/30 h = 8.3 km h^{-1} = 2.3 m s^{-1}), which is reasonable considering that the katabatic drainage flows from Byrd, Mulock, and Skelton glaciers tend to diverge over the ice shelf and slow down. The slight clockwise rotation at AWS 07 as the wind speed increases confirms this propagation. Notice that the wind speed at AWS 07 is, in general, slightly stronger than that at AWS 15 and much stronger than the propagation speed inferred above. This is due to the blocking effect of Ross Island on the airflow. The wind field at Williams Field presents a more complex situation due to Minna Bluff and White and Black islands to the south (see Fig. 2). These factors may contribute to the timing difference (6 h) between the minima at Williams Field and AWS 07 (0000 LST vs 0600 LST).

Above the surface level at Williams Field, the wind speeds present a similar pattern to AWS 07 (Fig. 9). The maxima are in the late afternoon and the minima in the morning.

4. Northwest wind events

In addition to studies of the blocking effect of Ross Island and Hut Point peninsula, the sodar wind data can be used to investigate the breakdown of the prevailing wind pattern, a topic that has received little attention. The wind rose (Fig. 12) at Scott Base (Fig. 1b) shows the prevailing wind direction from the northeast as a consequence of the blocking effect of Hut Point peninsula, a secondary peak from the southeast due to wind flow over Hut Point peninsula, and some winds from the northwest that represent the breakdown of the prevailing wind pattern. The surface wind rose at McMurdo Station (Sinclair 1982) also shows a similar pattern except that the northwest component at Scott Base is replaced by northerly components. This difference was investigated by Sinclair (1982) and was believed due to the local topographic influences (Fig. 1b). Surface northwesterly winds at the sodar site are weak in comparison to those shown on the sodar records. For most cases, the surface wind remained weak from the northeast or calm while northwest winds appeared above the 75-m height; for example, in Fig. 13, air at the surface remained calm while northwesterly flow was present aloft. Adverse weather—for example, snow or blowing snow with low visibility (five out of eight events)—was encountered during most of the northwest wind events. As discussed earlier, the prevailing wind in the Ross Island area is primarily due to katabatic drainage from Byrd, Mulock, and Skelton glaciers. The possible cause for the breakdown of the prevailing wind is a change of the propagation direction of the katabatic flow under the influence of meso- and synoptic-scale pressure systems. Such directional changes have been pointed out by Bromwich (1989). Figure 6 of that paper shows several types of propagation patterns but does not address the causes for such variations. In comparison to the interior of East Antarctica, the Ross Island area is situated near the coastal margins where meso- and synoptic-scale disturbances frequently occur, and these can deflect the katabatic winds that usually blow northward along the Transantarctic Mountains. With information from sodar measurements, AWS observations, satellite images, McMurdo rawinsonde data, and 500-hPa and sea level pressure analyses prepared by the Australian Bureau of Meteorology, two well-defined cases have been analyzed.

a. Case 1

A northwest wind was observed at McMurdo Station (unfortunately Scott Base conducts only once-daily

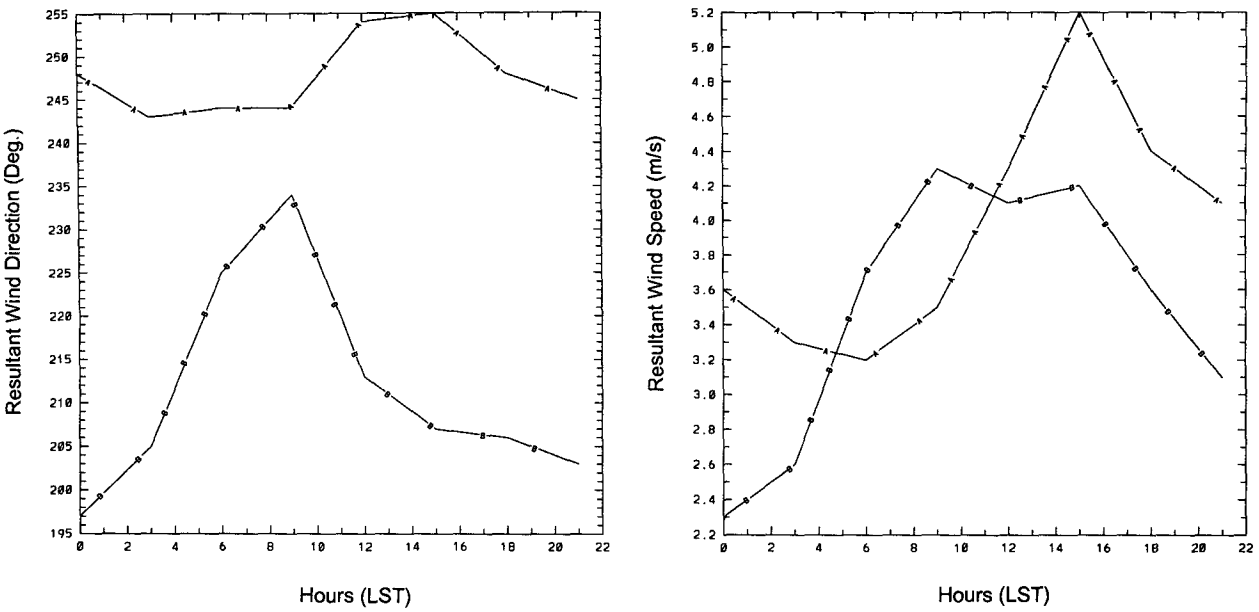

FIG. 11 (a) Diurnal variation of resultant wind direction at AWS 07 and 15. Lines A and B represent AWS 07 and 15, respectively. (b) Same as (a) but for resultant wind speed.

observations) from 1200 LST 19 October to 0300 LST 20 October. The wind was not observed at the surface level at Williams Field probably due to the blocking effect of Hut Point peninsula, which forced the airflow to rise over it. The sodar did show stronger northwesterly winds compared to those measured at McMurdo Station.

The evolution of the event can be described as follows. At 0000 LST 18 October, the 500-hPa analysis (Fig. 14a) showed that Ross Island area was under the influence of a low system centered over the Amundsen Sea. An isolated high center was over East Antarctica between the South Pole and Vostok Station, and an offshore ridge was located to the north of Adélie Land and was moving slowly to the east. Twelve hours later (Fig. 14b), the isolated high merged with the offshore ridge and started to weaken. Surface pressure also decreased over the Ross Sea/Ross Ice Shelf, but the falls were not uniform with larger values to the south of Ross Island. Such nonuniform pressure decreases created a surface pressure ridge in the Ross Island area (Fig. 15a) that extended from the north and was as-

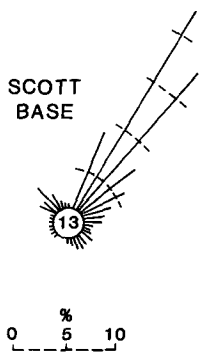

FIG. 12. Wind rose at Scott Base based on observations from 1966 to 1977 (after Sinclair 1982). The length of each line is proportional to the frequency of winds from that direction. The number in the circle is the percentage of calms.

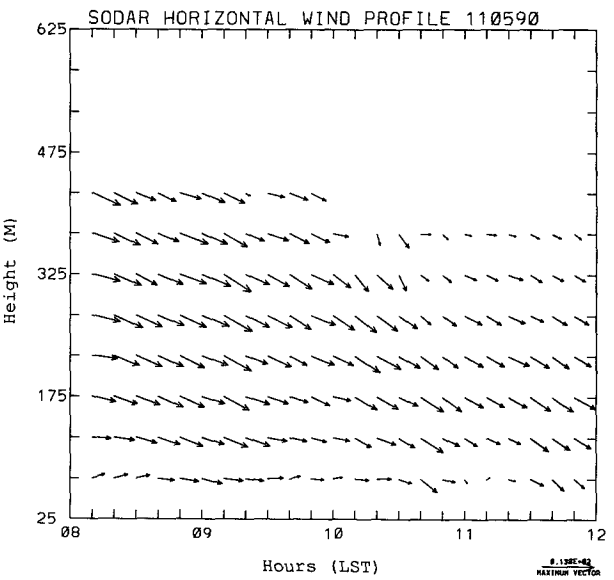

FIG. 13. An example of a northwest wind event between 0800 and 1200 LST 5 November 1990.

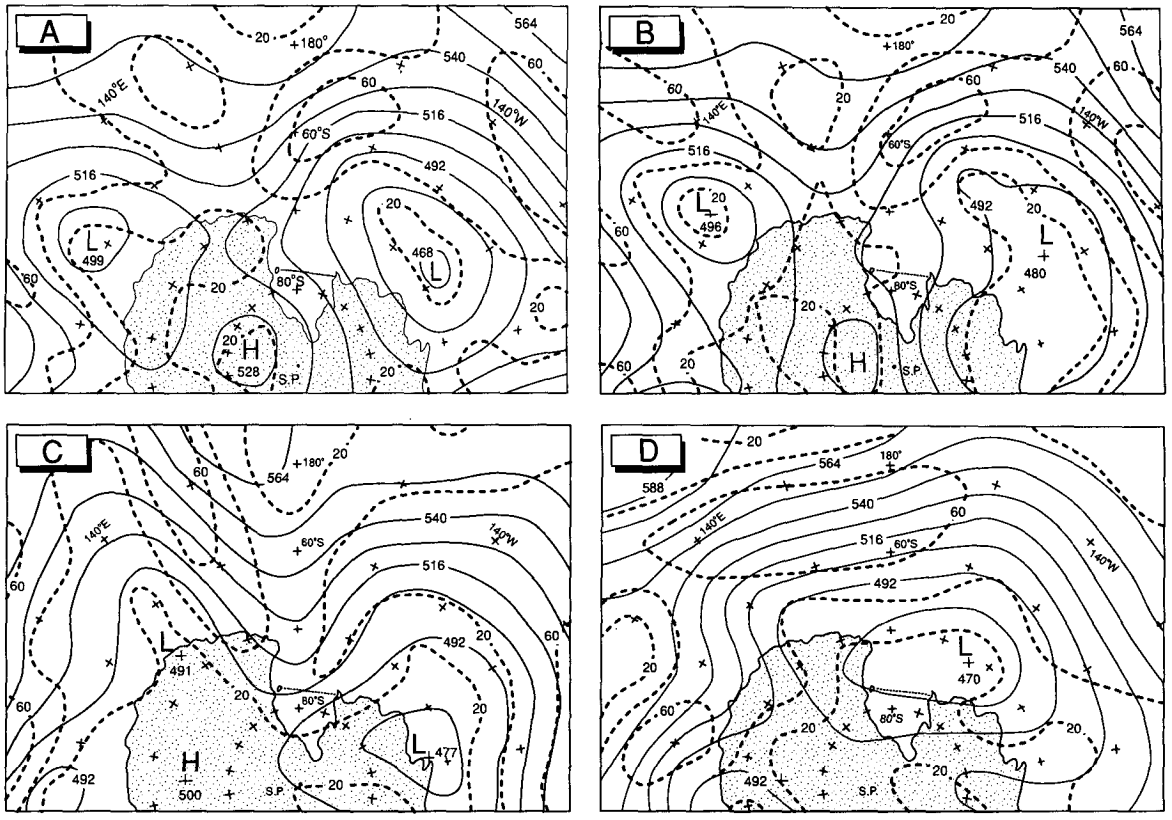

FIG. 14 (a) 500-hPa analysis for case 1 at 0000 LST 18 October prepared by the Australian Bureau of Meteorology. Contours (solid) in geopotential dekameters and isotachs (dashed) in knots. (b) Same as (a) but for 1200 LST 18 October. (c) Same as (a) but for 1200 LST 20 October. (d) Same as (a) but for case 2 at 1200 LST 26 October.

sociated with the southward extension of the 500-hPa ridge. As the surface ridge built up, the katabatic drainage flow started at 2100 LST 18 October to change its usual northeastward propagation direction, being steered by the local pressure field associated with the mesoscale low near Byrd Glacier. This is shown in Fig. 16a by the wind direction at AWS 24 turning clockwise. The genesis of mesoscale lows near Byrd Glacier has been studied recently (Bromwich 1991; Carrasco and Bromwich 1991). It was found that the sufficient conditions for genesis are horizontal temperature gradients in the boundary layer (called boundary-layer baroclinic zones) formed by the katabatic drainage flows from Byrd, Mulock, and Skelton glaciers and a weak surface trough. The katabatic drainage flows were confirmed by the katabatic signatures on thermal infrared satellite images (Bromwich 1989). The differential falls of surface pressure along the Transantarctic Mountains created a weak surface trough near Byrd Glacier. As the mesoscale low formed, the wind direction at McMurdo Station turned to the northwest (Fig. 16a). Figures 16a and 16b show that the ridge and the change of the katabatic drainage flow direction (turns clockwise) are associated with the formation of the northwesterly wind in the Ross Island area. The pressure analysis (Fig. 15a) indicates that the geostrophic wind direction near Ross Island was from the north. Deflection of this airflow around the local terrain of Ross Island (Fig. 1b) would give rise to northwesterly winds at Williams Field. The McMurdo radiosonde at 0000 LST 20 October showed that the surface northwesterly winds extended to about the 750-m height, which matched that in the sodar data. Above that level, the wind direction was uniformly from the southwest associated with the 500-hPa ridge. Apparently, the whole ridge system tilted toward the west with height.

Between 0000 and 1200 LST 20 October, the 500-hPa ridge axis crossed the Ross Island area (Fig. 14c). Prior to and during this time, the surface ridge moved eastward and weakened, and the prevailing wind resumed (Fig. 16a).

b. Case 2

The northwesterly wind started at 0400 LST 26 October and ended at 1500 LST 26 October. At 2339 LST 25 October, the prelude to this event was mesoscale ridging from Mulock and Skelton glaciers all the way to AWS 07, as in the average situation described by Bromwich (1991). During the last 24 h, a weak

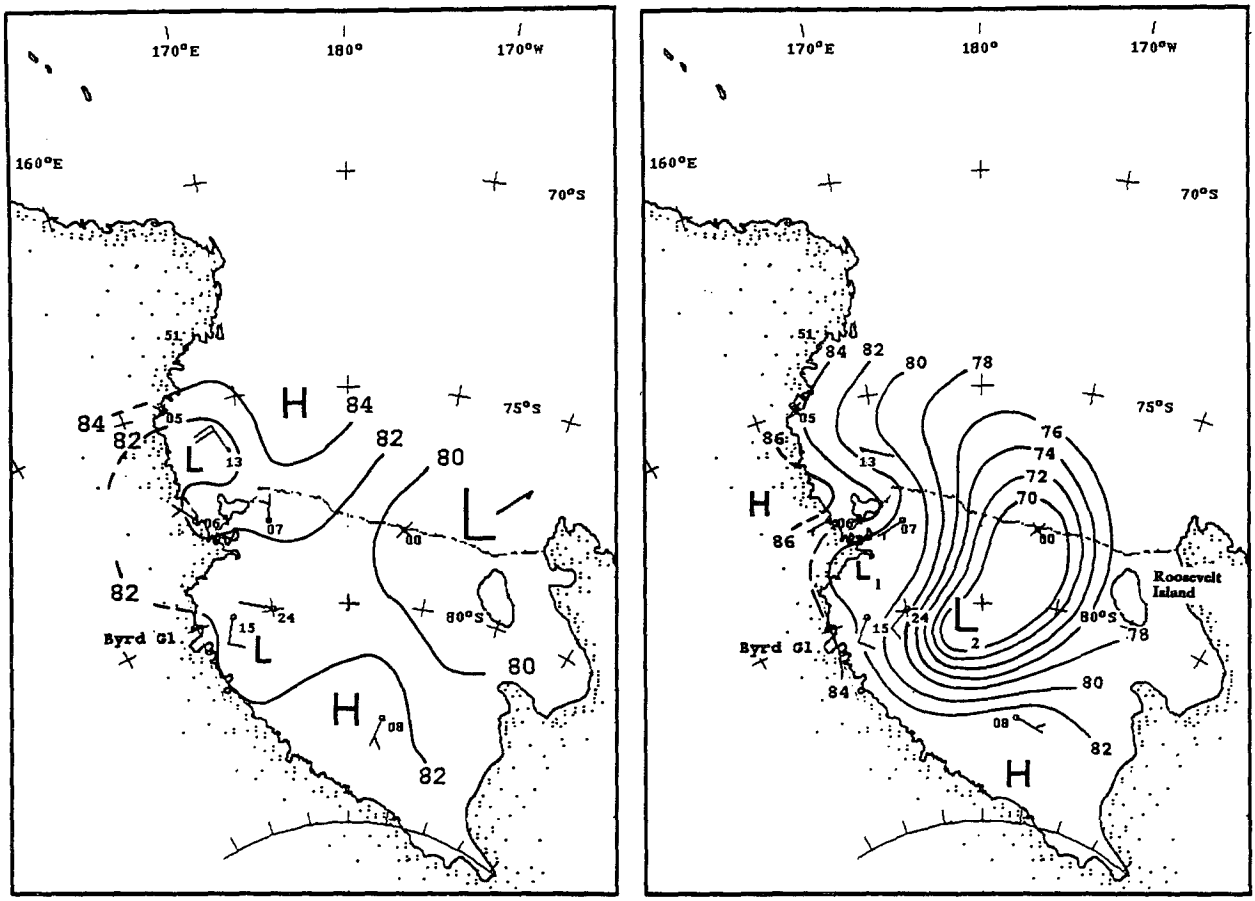

FIG. 15. (a) Sea level pressure analysis for case 1 at 2305 LST 19 October. Conventional plotting convention used for winds. Solid lines are sea level isobars (82≡982 hPa). (b) Same as (a) but for case 2 at 0435 LST 26 October.

dissipating mesoscale cyclone (L_1) had moved just to the south of AWS 07 from the center of the Ross Ice Shelf. At this time, a subsynoptic-scale cyclone (L_2) developed on a synoptic-scale front just to the northwest of Roosevelt Island. According to the AWS and satellite imagery analysis at 0435 LST 26 October (Fig. 15b), cyclone L_2, which was located near Roosevelt Island, had moved to just east of AWS 24, being steered by the general flow regime. This subsynoptic cyclone contained abundant moisture, and spiral clouds were clearly shown on the infrared satellite images. As a result, the area near AWS 24 and 15 was under the influence of the subsynoptic cyclone L_2 (Fig. 15b) and the katabatic winds from Byrd, Mulock, and Skelton glaciers were likely steered well to the east of Ross Island. The mesoscale ridge was displaced to the northwest. Although not evident from the mostly overcast satellite image, it is likely that the weak, nearly stationary mesoscale cyclone L_1 and the displaced mesoscale ridge combined to produce westerly geostrophic flow toward Ross Island. Northwesterly winds appeared at McMurdo Station, probably as a result of airflow deflection around the island. At 0615 LST 26 October, the subsynoptic cyclone started moving toward the Ross Island area. As cyclone L_2 approached, the northwest wind speeds below 250-m height at Williams Field increased due to the locally strengthening geostrophic winds; above that level, the sodar winds became chaotic because the signals were greatly reduced due to noise generated by the strengthening surface winds. At 1200 LST 26 October, a 9 m s^{-1} surface wind from the northwest was observed at Williams Field, and northerly winds were recorded at McMurdo Station. Sodar records showed a maximum northwest wind speed of 13 m s^{-1} at 76-m height. The approach of cyclone L_2 also generated snowfall and greatly reduced horizontal visibilities in the Ross Island area. Observations at McMurdo Station showed 20 miles of horizontal visibility before the wind speed increase and three-quarters of a mile afterward due to blowing snow. At 1500 LST 26 October, wind direction from both sodar and surface observations at Williams Field switched from northwest to southwest all the way from the surface to 500-m height as cyclone L_2 moved much closer to Ross Island, and presumably mesoscale cyclone L_1 moved to the northeast. As a result, the Ross Island area was under

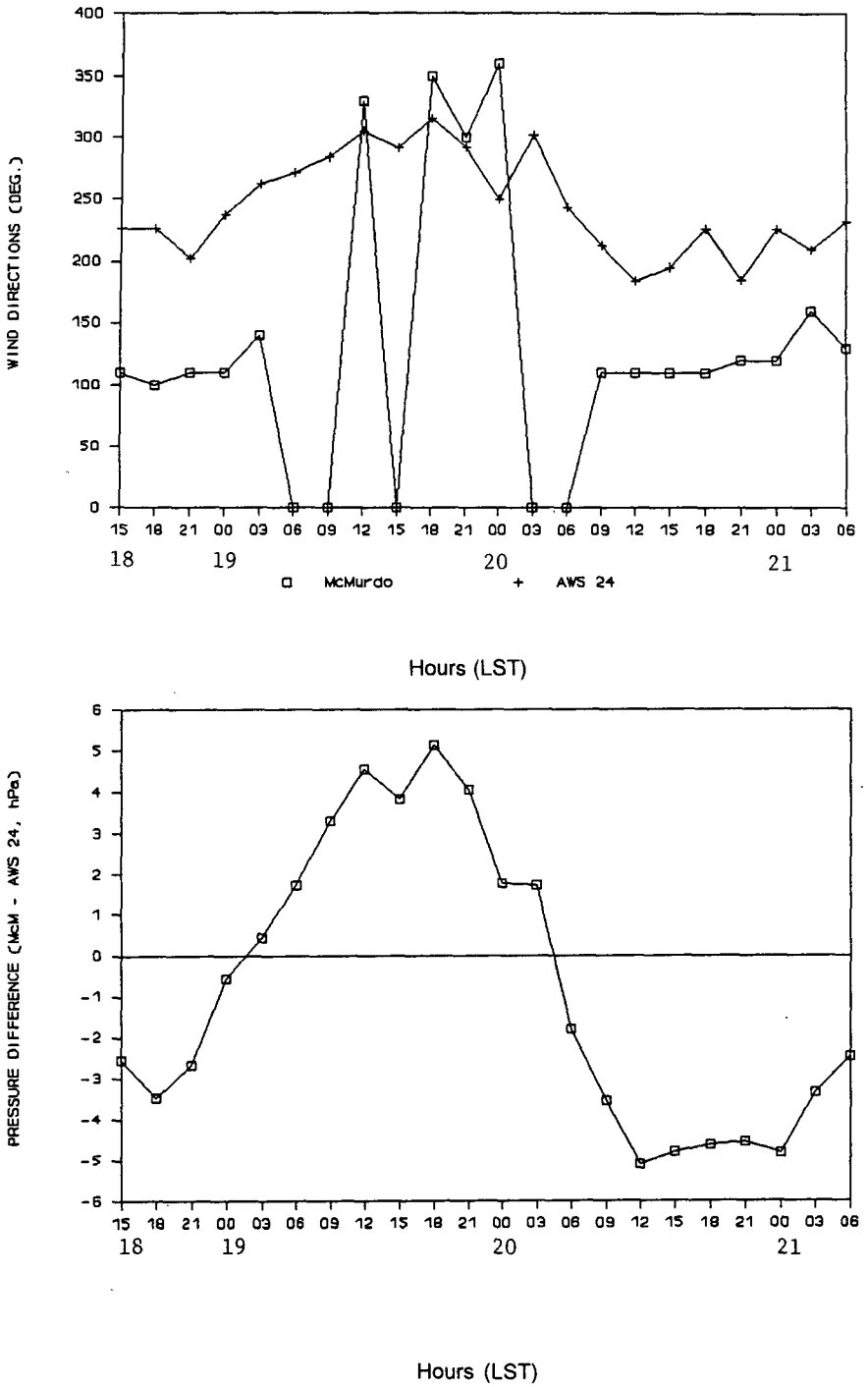

FIG. 16. (a) Wind directions at McMurdo Station and AWS 24, starting from 1500 LST 18 October 1990 for case 1. (b) Sea level pressure difference between McMurdo Station and AWS 24 for the same period.

the influence of the subsynoptic cyclone's southerly airflow. Due to poor weather that made the rawinsonde launch at McMurdo Station impossible, the vertical structure of the northwest wind is not known. Before the wind noise contamination greatly limited the vertical range, the sodar data showed that the depth of the northwest winds was quite shallow, below 500 m. During the event, the 500-hPa analysis (Fig. 14d) showed

that the Ross Island area was under the influence of a low system centered over the Amundsen Sea (isohypses cross the Ross Island area from the southeast to northwest). This suggests that the airflow at 500 hPa over the Ross Island area was dominated by southeasterly winds.

5. Conclusions

A clockwise horizontal wind direction rotation due to the blocking effect of Hut Point peninsula is confirmed by sodar wind data collected during this campaign. The 3-h resultant wind direction profile indicates that the wind direction rotation has a diurnal variation. A well-defined pattern is present during most of the day as a result of increasing wind speed and a Froude number that is far less than that obtained by O'Connor and Bromwich (1988) for airflow around Hut Point peninsula. A less well-defined pattern is found from 0300 to 0900 LST, partially due to the decrease of wind speed and consequently, more variable wind directions. A low-level jet, formed as a result of the blocking effect of Hut Point peninsula, is also confirmed by the sodar wind analysis. The diurnal variation of the airflow near the Ross Island area is due to the propagation of katabatic winds primarily from Byrd Glacier and secondarily from Mulock and Skelton glaciers. This leads to maximum surface wind speeds in the Ross Island area in the late afternoon and minimum speeds in the morning; for the minimum speeds there is a 6-h phase lag between the surface and the rest of the boundary layer. The katabatic wind propagation also makes the wind direction rotate clockwise with height. The shallow convective mixing layer, although it existed during most daytime hours, had limited effect on the boundary-layer behavior in this early austral summer period. Further explanation of the differences between surface and higher-level winds requires a better description of the vertical structure of the upstream airflow and of the effect of surrounding topography; one approach would be to deploy more sodars and temperature profilers.

The appearance of northwesterly winds represents the breakdown of the prevailing northeast or southeast winds due to changes in the broad-scale atmospheric circulation and often brings adverse weather to the Ross Island area. During such events, the prevailing upstream katabatic drainage flow either changed its direction or remained weak under the influence of meso- or synoptic-scale pressure gradients. The topographic setting of Ross Island allows meso- or synoptic-scale disturbances to penetrate into the area from the north, east, and south under the control of the broadscale circulation. The two cases showed that the northwesterly winds were generated by very localized geostrophic flows from the north through the west that are deflected by the topography of Hut Point peninsula. These localized pressure features result from the impact of the large-scale circulation on mesoscale lows and highs. The participation of mesoscale and subsynoptic-scale cyclones in these events explains why they are often associated with adverse weather.

The sodar, in conjunction with AWS and satellite imagery, proved to be an effective tool for probing the vertical structure and behavior of the stable planetary boundary layer. For example, without Doppler sodar wind data, the blocking effect of the Hut Point peninsula and the diurnal variation of the boundary-layer wind could not have been adequately studied.

Acknowledgments. The field program and research were sponsored by National Science Foundation Grant DPP-8916921 to David H. Bromwich. The satellite imagery was recorded by U.S. Navy personnel at McMurdo Station and obtained from Robert Whritner of the Arctic and Antarctic Research Center at Scripps Institution of Oceanography (NSF Grant DPP-8815818). The AWS data were obtained from Charles Stearns of the Department of Atmospheric and Oceanic Sciences at the University of Wisconsin—Madison (NSF Grants DPP-8606385, DPP-8818171, and DPP-9015586).

REFERENCES

Argentini, S., G. Mastrantonio, G. Fiocco, and R. Ocone, 1992: Complexity of the wind field as observed by a sodar system and by automatic weather stations on the Nansen Ice Sheet, Antarctica, during summer 1988–89: Two case studies. *Tellus,* **44B,** 422–429.

Bromwich, D. H., 1989: Satellite analyses of Antarctic katabatic wind behavior. *Bull. Amer. Meteor. Soc.,* **70,** 738–749.

——, 1991: Mesoscale cyclogenesis over the southwestern Ross Sea linked to strong katabatic winds. *Mon. Wea. Rev.,* **119,** 1736–1752.

——, J. F. Carrasco, and C. R. Stearns, 1992: Satellite observations of katabatic-wind propagation for great distances across the Ross Ice Shelf. *Mon. Wea. Rev.,* **120,** 1940–1949.

——, Y. Du, and T. R. Parish, 1994: Numerical simulation of winter katabatic winds from West Antarctica crossing Siple Coast and the Ross Ice Shelf. *Mon. Wea. Rev.,* submitted.

Carrasco, J. F., and D. H. Bromwich, 1991: A case study of katabatic wind-forced mesoscale cyclogenesis near Byrd Glacier. *Antarctic J., U.S.,* **26**(5), 258–261.

Hall, F. F., and E. J. Owens, 1975: Atmospheric acoustic echo sounding investigations at the South Pole. *Antarct. J. U.S.,* **10,** 191–192.

Keller, L. M., G. A. Weidner, and C. R. Stearns, 1991: *Antarctic Automatic Weather Station Data for the Calendar year 1990.* Department of Meteorology, University of Wisconsin, 383 pp. [Available from the Department of Atmospheric and Oceanic Sciences, 1225 W. Dayton St., Madison, WI 53706.]

Kitabayashi, K. 1977: Wind tunnel and field studies of stagnant flow upstream of a ridge. *J. Meteor. Soc. Japan,* **55,** 193–203.

Liu, Z., and D. H. Bromwich, 1992: Acoustic remote sensing study of boundary layer blocking near Ross Island, Antarctica. Preprints, *Third Conf. on Polar Meteorology and Oceanography,* Portland, OR, Amer. Meteor. Soc., J29–J32.

——, J. K. Geer, and D. H. Bromwich, 1991: A boundary layer study near Ross Island using acoustic remote sensing. *Antarct. J. U.S.,* **26**(5), 254–256.

Mastrantonio, G., R. Ocone, and G. Fiocco, 1988: Acoustic remote sensing of the Antarctic boundary layer. *Proc. First Workshop Italian Research on Antarctic Atmosphere,* M. Colacino, G.

Giovanelli, and L. Stefanutti, Eds., Italian Physical Society, Bologna, 137–144.

Neff, W. D., 1981: An observational and numerical study of the atmospheric boundary layer overlying the East Antarctic ice sheet. NOAA Tech. Memor. ERL WPL67, 272 pp. [Available from NOAA/Wave Propagation Laboratory, 325 Broadway, Boulder, CO 80304.]

O'Connor, W. P., and D. H. Bromwich, 1988: Surface airflow around Windless Bight, Ross Island, Antarctica. *Quart. J. Roy. Meteor. Soc.*, **114,** 917–938.

Parish, T. R., and D. H. Bromwich, 1986: The inversion wind pattern over West Antarctica. *Mon. Wea. Rev.*, **114,** 849–860.

——, and ——, 1987: The surface windfield over the Antarctic ice sheets. *Nature,* **328,** 51–54.

——, and ——, 1991: Continental-scale simulation of the Antarctic katabatic wind regime. *J. Climate,* **4,** 135–146.

——, P. Pettre, and G. Wendler, 1993: A numerical study of the diurnal variation of the Adélie Land katabatic wind regime. *J. Geophys. Res.*, **98,** 12 933–12 947.

Schwerdtfeger, W., 1984: *Weather and Climate of the Antarctic.* Elsevier Science Publishers, 261 pp.

Sinclair, M. R., 1982: Weather observations in the Ross Island area, Antarctica. New Zealand Meteorological Service, Tech. Note No. 253, 36 pp. [Available from the Director, New Zealand Meteorological Service, P.O. Box 722, Wellington, New Zealand.]

Slotten, H. R., and C. R. Stearns, 1987: Observations of the dynamics and kinematics of the atmospheric surface layer on the Ross Ice Shelf, Antarctica. *J. Climate Appl. Meteor.*, **26,** 1731–1747.

Stearns, C. R., and G. A. Weidner, 1990: Wind speed events and wind direction at Pegasus site during 1989. *Antarct. J. U.S.*, **25**(5), 258–262.

Stull, R. B., 1988: *An Introduction to Boundary Layer Meteorology.* Kluwer Academic Publishers, 666 pp.